J. Am. Ceram. Soc., 93 [8] 2167–2170 (2010)
DOI: 10.1111/j.1551-2916.2010.03704.x

journal

Investigation on Thermal Conductivity of Aluminum Nitride Ceramics by FT-Raman Spectroscopy

Hyeon-Keun Lee and Do Kyung Kim*,†

Department of Materials Science and Engineering, Korea Advanced Institute of Science and Technology (KAIST), Yuseong-gu, Daejeon 305-701, Korea

FT-Raman spectroscopy was used to characterize the thermal conductivity of yttria-doped polycrystalline aluminum nitride (AlN) ceramics. Specimens with different thermal conductivity were prepared using sintering additives of different size, content, and mixing method. The broadening of the Raman mode is caused by point defects and impurities, which affect the thermal conductivity of the AlN grains (lattice thermal conductivity). The width of the Raman line was related to the *c*-axis lattice parameter contraction, which was caused by aluminum vacancies produced by various defects. A correlation is suggested between the width of the E_2 (high) phonon mode and the lattice thermal conductivity of AlN ceramics.

I. Introduction

Aluminum nitride (AlN) has gained a great deal of importance in several device applications ranging from electronic substrates to semiconductor manufacturing equipment applications. The importance of AlN is based on its unique properties including: a wide band gap ($E_g = 6.2$ eV at room temperature), high thermal conductivity, low thermal expansion coefficient, high mechanical properties, and chemical inertness.[1–3] In particular, its high thermal conductivity coupled with low thermal expansion (similar to Si), high electrical resistivity, and high plasma resistance make it a promising candidate for electronic substrates, such as electrostatic chucks.[4–6]

In the case of insulators and semiconductors, thermal conduction is exclusively by the diffusion of phonons through the solid. Therefore, phonons govern the thermal properties of the solid, which are largely influenced by the nature and number of native defects and impurities in the materials. In single-crystal and polycrystalline AlN, the most dominant defects are oxygen-related defects that consist of oxygen substitutions for nitrogen (O_N), aluminum vacancies (V_{Al}), and O_N–V_{Al} complexes. The large accommodation of oxygen can influence the thermal conductivity of AlN. However, the role of oxygen and oxygen-related defects on the thermal conductivity of AlN has not been clearly understood, because of the poor treatment of anharmonic effects, which occur together with the defect effects in controlling phonon lifetimes.[7,8]

Raman spectroscopy is a very useful tool for the study of phonon dynamics and phonon interactions, as well as the factors influencing them. The width of a Raman line can be associated with the phonon mean free path.[9,10] If there are no strong stress gradients in the material, the measured full width at half maximum (FWHM) can be associated with point defect scattering. Recently, Bergman *et al.*[11] reported that micro-Raman linewidths become about 50% broader by the incorporation of Si and C impurities in the AlN wurtzite structure. McCullen *et al.*[12] found that the broadening of E_2 (high) and E_2 (low) Raman lines measured by micro-Raman spectroscopy is related to oxygen concentrations in the AlN film. From these studies, it can be assumed that defects and impurities in AlN cause Raman linewidth broadening. The broadening of the Raman linewidth is due to the combined effects of anharmonic decay, which determines the intrinsic linewidth, and point defect scattering.

In this work, a detailed FT-Raman spectroscopy study was carried out on yttria-doped polycrystalline AlN ceramics. The thermal conductivity of AlN grains calculated from bulk thermal conductivity was compared with the broadening of Raman linewidths caused by phonon scattering. In addition, the width of Raman lines of the E_2 (high) phonon were related to the oxygen-related defects and impurities, as measured from the lattice parameter through X-ray diffraction (XRD).

II. Experimental Procedure

Polycrystalline AlN ceramics were sintered to a high density using different powder sizes of yttria as a sintering additive. Commercially available high-purity AlN powder (Grade F, Tokuyama Soda, Tokyo, Japan, 0.85 wt% oxygen) was mixed with 1, 3, and 5 wt% micrometer-sized yttria (Y_2O_3, purity 99.99%, Alfa Products, Ward Hill, MA, primary particle size: 10 μm) or nanosized yttria (Y_2O_3, Sigma-Aldrich, St. Louis, MO, primary particle size: 50 nm; specific surface area: 45 m^2/g) each separately, and ball milled for 24 h in ethanol using zirconia media. In the case of the use of a yttria coating as sintering additive, AlN powder was dispersed in a calculated amount of yttrium nitrate ($Y(NO_3)_3$, purity 99.9%, Aldrich) dissolved in ethanol and coated using diethylamine (purity 99.0%, Junsei Chemical, Tokyo, Japan) as a precipitating agent. After subsequent drying and granulation, the powders were uniaxially pressed into 20-mm-diameter disks under a pressure of 30 kg/cm^2 and isostatically pressed at 200 MPa. The pellets were sintered via a pressure-less sintering in an Astro furnace (Astro Thermal Technology, Santa Barbara, CA) at 1900°C for 3 h in an N_2 atmosphere.

The phase and crystal structure were characterized by XRD (Rigaku, D/MAX-IIIC, Tokyo, Japan) with Cu$K\alpha$ radiation ($\lambda = 0.15406$ nm at 40 kV and 45 mA). The fracture surface of sintered pellets was characterized by scanning electron microscopy (FE-SEM Philips XL30 FEG, Eindhoven, the Netherlands). The FT-Raman spectra were recorded for the pellets sintered with different sizes of yttria using a Bruker Optics RFS 100/S FT-Raman Spectrometer (Bruker Instruments Inc., Billerica, MA) using a diode pumped Nd:YAG laser with a continuous-wave output at 1064 nm (785 and 1064 dual-channel

K. Watari—contributing editor

Manuscript No. 27247. Received December 23, 2009; approved February 3, 2010.
This study was supported by a grant from the Fundamental R&D Program for Core Technology of Materials funded by the Ministry of Commerce, Industry and Energy, Republic of Korea. This work was also partially supported by the National Research Foundation of Korea (NRF) grant funded by the Korea government (MEST) (2008-0062206).
*Member, The American Ceramic Society.
†Author to whom correspondence should be addressed. e-mail: dkkim@kaist.ac.kr

laser). The detector is a liquid-nitrogen-cooled Ge/Si detector. The measurement was performed with a 785-nm line laser and the incident laser beam providing a beam spot of approximately 1 mm in diameter on the sample at room temperature. The acquisition time for each Raman spectrum was approximately 10 min depending on the sample. The Raman shift range acquired was from 200 to 1000 cm^{-1}. The nominal spectral resolution for the FT-Raman measurements was 1 cm^{-1}. The bulk thermal conductivity was measured by the laser flash method (LFA 447 Nanoflash, Netzsch Instruments Inc., Burlington, VT).

III. Results and Discussion

Figure 1(a) shows a typical backscattered SEM image of the fracture surface of a 5 wt% nanosized yttria–AlN pellet sintered at 1900°C for 3 h. The micrograph images of sintered pellets revealed highly dense ceramics with negligible porosity, and a clearly resolved uniform dispersion of the second phase located along the grain boundaries. The average thickness of the secondary phase was about 0.5–1 μm. XRD patterns of the yttria–AlN pellets sintered at 1900°C (not shown here) confirmed a wurtzite structure along with yttrium aluminate as a second phase. The thermal conductivities of polycrystalline AlN ceramics with different wt% (1, 3, and 5 wt%), size (micro and nano), and mixing method (ball milling and chemical coating) of sintering additives[13,14] were in the range 95–190 W/mK, as measured by the laser flash method. Different size and mixing method of yttria were used to vary the thermal conductivity of AlN as changing the distribution of the sintering additives.

A typical FT-Raman spectrum is shown in Fig. 1(b) of the 5 wt% nanosized yttria–AlN pellet sintered at 1900°C for 3 h. For all the sintered AlN pellets, the peaks observed at about 612, 658, and 666 cm^{-1} can be assigned to the A_1(TO), E_2 (high), and E_1 (TO) modes of AlN, respectively.[15] Among the active Raman modes of AlN, nonpolar E_2 (low) and E_2 (high) modes mainly correspond to the vibrations of the Al sublattice and N atoms, respectively.[16–18] The E_2 (high) mode was the strongest of the allowed modes in the wurtzite structure of the polycrystalline AlN ceramics and it was used to relate the peak broadening to defects or impurities. In order to calculate the Raman linewidth, i.e., FWHM of the E_2 (high) mode peak, the peak was fitted using a Lorentzian function because the line shape of the phonon mode can be approximated by a Lorentzian.[11] The linewidths of the E_2 (high) mode measured for the different AlN pellets ranged from 6.5 to 7.9. These values are greater than the linewidth value of 3 cm^{-1} for an AlN single crystal of high perfection.[18] This means that the polycrystalline AlN ceramics used in this study contained a considerable concentration of scattering sources of phonons, which were related to oxygen defects or some impurities, compared with single crystalline AlN. In polycrystalline AlN ceramics, oxygen-related defects and some impurities exist in the AlN grains. Oxygen-related defects are formed by substitution of oxygen atoms for N atoms. This substitution affects the local crystal field due to alloy potential variations resulting from the loss of the translational constant, leading to the breakdown of the wave vector (the $q = 0$ Raman selection rule). Thus, the broadening in the Raman peaks observed is a result of the scattering from the whole Brillouin zone.[12] The Si impurity, which is one of the major impurities of AlN ceramics in place of the Al ion, is a negligible scatterer of phonons. However, there should be a cation vacancy for every three Si ions, and this defect could be a phonon scattering source.[19] Therefore, the width of the Raman line will be affected when oxygen occupies an N site or an impurity arises at the site of an Al ion.

In order to know the relationship between the Raman linewidth and various defects in AlN grains, lattice parameter measurements were carried out by the X-ray diffraction. As mentioned above, defects and impurities in AlN cause the formation of aluminum vacancies due to the charge neutrality constraint. The AlN lattice contraction is predominantly due to the formation of aluminum vacancies, and we were able to analyze defect concentrations by measuring the *c*-axis lattice parameter from X-ray data by using the Cohen least squares method.[16,17,20] The linewidths of the E_2 (high) mode compared with the *c*-axis lattice parameter are plotted in Fig. 2. The inset in Fig. 2 shows the (205) X-ray diffraction peaks of the three selected samples, which had Raman linewidths of 6.5, 7.3, and 7.9 cm^{-1}, respectively. The samples with greater Raman linewidths of the E_2 (high) mode exhibited (205) peak shifts toward lower 2θ angles and confirmed that increasing numbers of aluminum vacancies were formed by point defects and impurities. As a result, Fig. 2 reveals a correlation between the Raman linewidth and the *c*-axis lattice parameter affected by the amount of aluminum vacancies. A similar correlation has been found previously in AlN films.[10]

The linewidths of the E_2 (high) Raman mode are compared with the lattice thermal conductivity as shown in Fig. 3. The lattice thermal conductivity of the pellets used in this study was calculated from the bulk thermal conductivity using Buhr and Muller's interconnected second-phase model.[13,21] In Fig. 3, it is

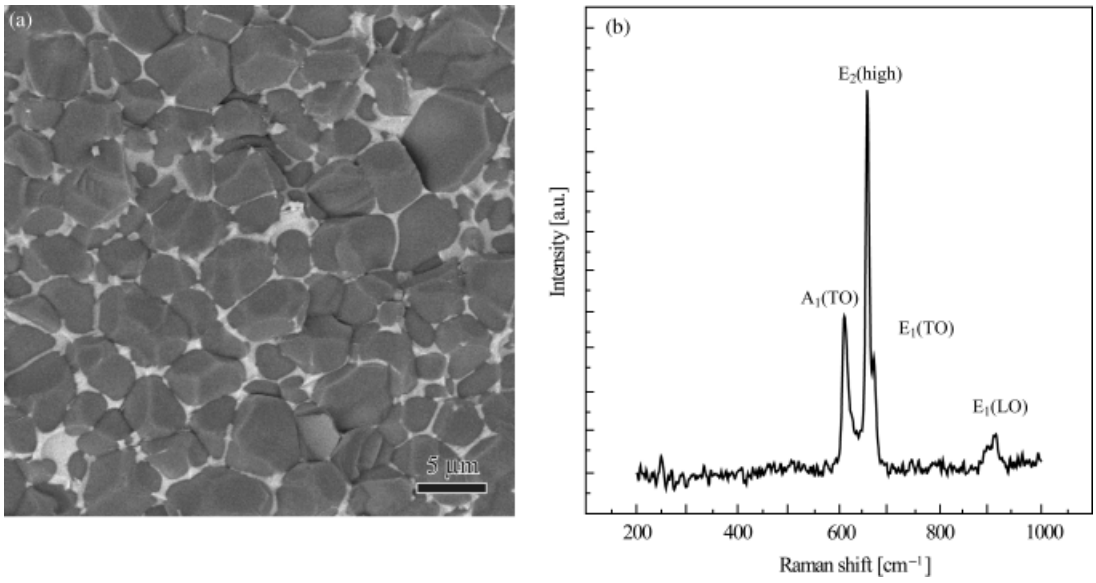

Fig. 1. (a) Backscattered scanning electron microscopy image of the fracture surface of 5 wt% nanosized yttria–polycrystalline aluminum nitride (AlN) ceramics. (b) Raman spectrum of 5 wt% nanosized yttria–polycrystalline AlN ceramics by FT-Raman spectrometer.

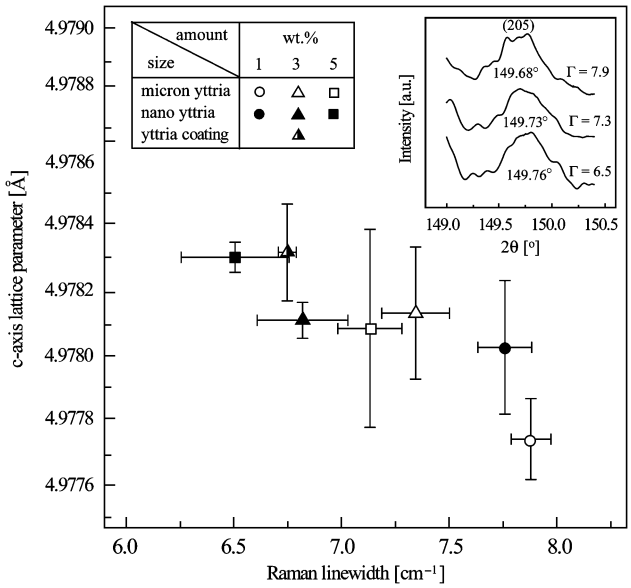

Fig. 2. Correlation between *c*-axis lattice parameter and Raman linewidth of the E_2 (high) mode. The inset shows the (205) diffraction peaks of three selected samples.

observed evidently that increasing the content of sintering additive increases the thermal conductivity. In general, the thermal conductivity of polycrystalline AlN ceramics is affected by two factors: the lattice (grain) thermal conductivity and the second-phase thermal conductivity. The lattice thermal conductivity is determined by defects, namely oxygen-related defects, or impurities within the AlN grain. The differences in grain size may not affect the lattice thermal conductivity because the phonon mean free paths were too small relative to the AlN grain sizes of 5–10 μm used in this study.[22] In order to investigate the effects of point defect scattering in AlN grains on thermal conductivity, the lattice thermal conductivity was considered. The width of the E_2 (high) mode shows a linear relationship with the lattice thermal conductivity in the range of thermal conductivity values used in this study. Considering the theoretical thermal conductivity (320 $W \cdot (m \cdot K)^{-1}$) of AlN, the linear fitting equation of the data can be represented as

$$K = 320 - \alpha(\Gamma - \beta) \quad (1)$$

where Γ is the Raman linewidth. The variables α and β are determined from a regression fit of the lattice thermal-conductivity results, and their values are $\alpha = 94\ W \cdot (m \cdot K \cdot cm)^{-1}$ and $\beta = 5.6\ cm^{-1}$. β is the Raman linewidth (FWHM) of the mode, which is the intrinsic linewidth caused by the effect of the anharmonic decay of AlN. The calculated intrinsic linewidth (β) values of the present work is larger than the value of 3 cm^{-1} for highly perfect single crystalline AlN measured by micro-Raman spectroscopy.[18] The intrinsic linewidth of polycrystalline AlN measured by FT-Raman spectroscopy can be broadened by scattering sources such as the second phase between AlN grains or grain boundaries, because of the large laser spot size and depth of focus of the FT-Raman spectrometer. Further detailed study on the intrinsic linewidth of polycrystalline materials is being carried out. In Eq. (1), we consider the point defect scattering effects in polycrystalline AlN ceramics by subtracting the β value from the Raman linewidth obtained.

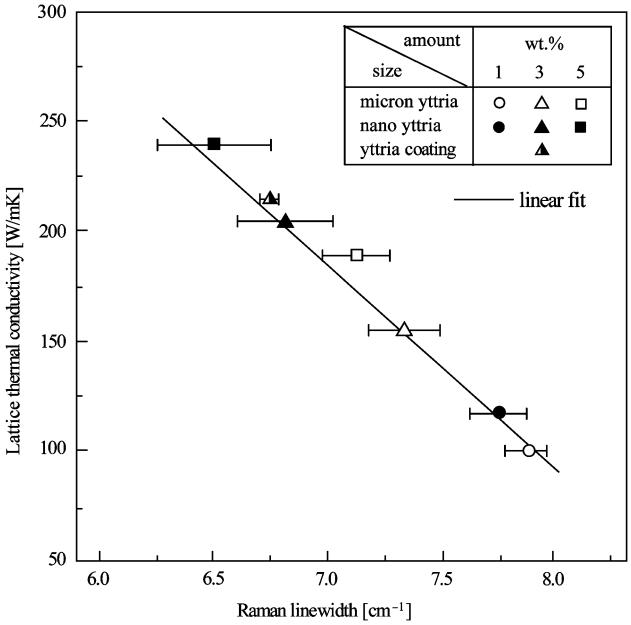

Fig. 3. Correlation between the lattice thermal conductivity normalized from measured thermal conductivity by the laser flash method and Raman linewidth of the E_2 (high) mode for the different wt% and sizes of yttria–polycrystalline bulk AlN ceramics.

IV. Conclusion

We have shown through FT-Raman spectroscopy that the width of the E_2 (high) mode has a linear relationship with the lattice thermal conductivity of polycrystalline AlN ceramics and that the width of the E_2 (high) mode is related to the lattice parameter contraction caused by various defects in the AlN grains. By measuring the width of the E_2 (high) Raman line in polycrystalline AlN ceramics, the thermal conductivity of AlN grains, which is affected by oxygen-related defects or impurities, could be estimated.

References

[1]G. A. Slack, R. A. Tanzilli, R. O. Pohl, and J. W. Vandersande, "The Intrinsic Thermal Conductivity of AlN," *J. Phys. Chem. Solids*, **48**, 641–7 (1987).
[2]R. Bachelard and P. Joubert, "Aluminum Nitride by Carbothermal Nitridation," *Mater. Sci. Eng. A—Struct. Mater*, **109**, 247–51 (1989).
[3]L. M. Sheppard, "Aluminum Nitride—A Versatile but Challenging Material," *Am. Ceram. Soc. Bull.*, **69** [11] 1801–12 (1990).
[4]L. Chouanine, M. Takano, F. Ashihara, and O. Kamiya, "Influence of the Surface Topography on the Micromechanical Properties and Performance of a CMP Finished AlN Component for Silicon Plasma Etching," *Adv. Fract. Failure Prev.*, **261–263** [Parts 1 and 2] 1599–604 (2004).
[5]S. Kume, M. Yasuoka, N. Omura, and K. Watari, "Effects of Annealing on Dielectric Loss and Microstructure of Aluminum Nitride Ceramics," *J. Am. Ceram. Soc.*, **88** [11] 3229–31 (2005).
[6]M. Watanabe, Y. Mori, T. Ishikawa, T. Iida, K. Akiyama, K. Sawabe, and K. Shobatake, "X-Ray Photoelectron Spectroscopy of Polycrystalline AlN Surface Exposed to the Reactive Environment of XeF_2," *Appl. Surf. Sci.*, **217** [1–4] 82–7 (2003).
[7]Q. L. Hu, T. Noda, H. Tanigawa, T. Yoneoka, and S. Tanaka, "The Oxygen-Related Defect Complexes in AlN Under Gamma Irradiation and Quantum Chemistry Calculation," *Nucl. Instrum. Methods Phys. Res. Sect. B*, **191**, 536–9 (2002).
[8]T. Mattila and R. M. Nieminen, "*Ab Initio* Study of Oxygen Point Defects in GaAs, GaN, and AlN," *Phys. Rev. B*, **54** [23] 16676–82 (1996).
[9]L. A. Falkovsky, J. M. Bluet, and J. Camassel, "Strain Relaxation at the 3C–SiC/Si Interface: Raman Scattering Experiments," *Phys. Rev. B*, **57** [18] 11283–94 (1998).
[10]V. Lughi and D. R. Clarke, "Defect and Stress Characterization of AlN Films by Raman Spectroscopy," *Appl. Phys. Lett.*, **89** [24] 241911 (2006).
[11]L. Bergman, D. Alexson, P. L. Murphy, R. J. Nemanich, M. Dutta, M. A. Stroscio, C. Balkas, H. Shin, and R. F. Davis, "Raman Analysis of Phonon Lifetimes in AlN and GaN of Wurtzite Structure," *Phys. Rev. B*, **59** [20] 12977–82 (1999).
[12]E. F. McCullen, J. S. Thakur, Y. V. Danylyuk, G. W. Auner, and L. W. Rosenberger, "Investigation of the Occupation Behavior for Oxygen Atoms in AlN Films Using Raman Spectroscopy," *J. Appl. Phys.*, **103** [6] 063504 (2008).
[13]W. J. Kim, D. K. Kim, and C. H. Kim, "Morphological Effect of Second Phase on the Thermal Conductivity of AlN Ceramics," *J. Am. Ceram. Soc.*, **79** [4] 1066–72 (1996).

[14]T. B. Jackson, A. V. Virkar, K. L. More, R. B. Dinwiddie, and R. A. Cutler, "High-Thermal-Conductivity Aluminum Nitride Ceramics: The Effect of Thermodynamic, Kinetic, and Microstructural Factors," *J. Am. Ceram. Soc.*, **80** [6] 1421–35 (1997).

[15]L. E. McNeil, M. Grimsditch, and R. H. French, "Vibrational Spectroscopy of Aluminum Nitride," *J. Am. Ceram. Soc.*, **76** [5] 1132–6 (1993).

[16]G. A. Slack, "Nonmetallic Crystals with High Thermal Conductivity," *J. Phys. Chem. Solids*, **34**, 321–5 (1973).

[17]J. H. Harris, R. A. Youngman, and R. G. Teller, "On the Nature of the Oxygen-Related Defect in Aluminum Nitride," *J. Mater. Res.*, **5** [8] 1763–73 (1990).

[18]M. Kuball, J. M. Hayes, Y. Shi, and J. H. Edgar, "Phonon Lifetimes in Bulk AlN and Their Temperature Dependence," *Appl. Phys. Lett.*, **77** [13] 1958–60 (2000).

[19]P. G. Klemens, "Effect of Point Defects on the Decay of the Longitudinal Optical Mode," *Physica B*, **316**, 413–6 (2002).

[20]M. U. Cohen, "Precision Lattice Constants from X-Ray Powder Photographs," *Rev. Sci. Instrum.*, **6** [3] 68–74 (1935).

[21]H. Buhr and G. Muller, "Microstructure and Thermal-Conductivity of AlN(Y_2O_3) Ceramics Sintered in Different Atmospheres," *J. Eur. Ceram. Soc.*, **12** [4] 271–7 (1993).

[22]K. Watari, K. Ishizaki, and T. Fujikawa, "Thermal Conduction Mechanism of Aluminum Nitride Ceramics," *J. Mater. Sci.*, **27** [10] 2627–30 (1992). □